Theoretical study of intramolecular vibrational relaxation of acetylenic CH vibration for $v=1$ and 2 in large polyatomic molecules $(CX_3)_3YCCH$, where X=H or D and Y=C or Si

A. A. Stuchebrukhov and R. A. Marcus
Arthur Amos Noyes Laboratory of Chemical Physics,[a] *California Institute of Technology, Pasadena, California 91125*

(Received 27 November 1992; accepted 8 January 1993)

Quantum calculations are reported for the intramolecular vibrational energy redistribution and absorption spectra of the first two excited states of the acetylenic CH stretch vibration in the polyatomic molecules $(CX_3)_3YCCH$, where X=H or D and Y=C or Si. Using approximate potential energy surfaces, comparison is made with the corresponding recent experimental spectra. It is found that a model of intramolecular vibrational relaxation based on the assumption of sequential off-resonance transitions via third and fourth order vibrational couplings (as opposed to direct high order couplings) is in agreement with experimental results on spectral linewidths. In a semiclassical limit this type of relaxation corresponds to a dynamic tunneling in phase space. It is shown that the local density of resonances of third and fourth order, rather than the total density of states, plays a central role for the relaxation. It is found that in the Si molecule an accidental absence of appropriate resonances results in a bottleneck in the initial stages of relaxation. As a result, an almost complete localization of the initially prepared excitation occurs. It is shown that an increase of the mass alone of the central atom from C to Si cannot explain the observed difference in the C and Si molecules. The spectral linewidths were calculated with the Golden Rule formula after prediagonalization of the relevant vibrational states which are coupled in the molecule to the CH vibration, directly or indirectly. For the spectral calculations, in addition to the direct diagonalization, a modified recursive residue generation method was used, allowing one to avoid diagonalization of the transformed Lanczos Hamiltonian. With this method up to 30 000 coupled states could be analyzed on a computer with relatively small memory. The efficiency of *C* programming language for the problem is discussed.

I. INTRODUCTION

In the present paper quantum calculations of intramolecular vibrational relaxation (IVR) of the acetylenic CH vibration in $(CX_3)_3YCCH$ molecules, where X=H, D and Y=C, Si, are reported. The study was motivated by the recent experimental results of Scoles, Lehmann, and collaborators.[1-2] (A brief review of recent experimental progress in overtone relaxation dynamics is given in Ref. 1 and references cited therein.) For these molecules extremely narrow, 10^{-1}–10^{-2} cm^{-1}, vibrational lines have been observed. The lines are believed to be homogeneously broadened. Such a small broadening means that an initially prepared excitation would remain localized for hundreds of thousands of vibrational periods of the CH vibration, indicating a nonclassical mechanism for relaxation responsible for the spectral broadening in these molecules.

The problem of numerical simulation of the quantum dynamics on the time scale of hundreds of picoseconds in large molecules is nontrivial. The total density of states involved in vibrational couplings should be of the order of several thousand states per cm^{-1} or higher, to have several spectral components in the interval of 10^{-2} cm^{-1}. Important anharmonic couplings can be of the order of 10 cm^{-1} or larger. In an energy window of 50 cm^{-1}, which is a minimum for such calculations, there would be more than 50 000 states to diagonalize. The computational problem of dealing with enormous basis sets in vibrational dynamics and spectroscopy of polyatomic molecules has been extensively discussed by Wyatt and co-workers.[3,4]

In the past there have been many theoretical studies of quantum and classical vibrational dynamics of overtones.[5-21] A comprehensive review of general theories of IVR in polyatomic molecules was presented recently by Uzer.[5] In the previous studies, however, primarily spectral features on the scale of 10–100 cm^{-1} were the focus of attention. The spectral resolution required to explain results of Refs. 1 and 2 must be at least 2 orders of magnitude higher.

The present analysis shows that the the vibrational relaxation occurs through a sequence of many intermediate off-resonant transitions until the appropriate high density of quasiresonant states is reached. The number of sequential virtual transitions required can be as large as ten or more in this treatment. Recently, we have shown[22] that this type of quantum dynamics involving many high order perturbation theory transitions in a semiclassical limit corresponds to a dynamic tunneling[22-27] in phase space. Some time ago Davis and Heller published a short qualitative paper,[24] which is directly related to this mechanism of relaxation. They noted that, even when the motion of a clas-

[a]Contribution No. 8752.

 0021-9606/93/086044-18$06.00

sical system is dynamically confined in phase space to a torus with some action variables $(I_1...I_s)$, different parts of the phase space might, however, be connected through tunneling. In large polyatomic molecules, such as those mentioned earlier, there are many quasidegenerate in energy tori $(I'_1...I'_s)$, which can can be coupled through dynamic tunneling to the "initial state" $(I_1...I_s)$, providing a tunneling mechanism for intramolecular relaxation. In this paper we, in fact, calculate a spectral width associated with this process in a quantum mechanical system.

One of the most striking experimental results of Refs. 1 and 2 is that the linewidth of the CH transition has seemingly no correlation with the total density of states. For example, the linewidth of the X=H, Y=Si compound is approximately ten times narrower than that of the X=H, Y=C compound. However, if one considered only the total density of states as the key factor in the broadening one would expect the opposite effect. Moreover, for the first overtone, $v=0\rightarrow 2$, the linewidth of the Si compound decreased by factor of 2 compared with that of the $v=0\rightarrow 1$ transition, while for the C compound it increased by factor of 2. The total density of states in both cases increases by 3 orders of magnitude. One possible explanation is that there is a heavy atom (Si) blocking effect,[28–34] although in this case the mass of Si seems to be still rather small to do much blocking. In the present paper we show that the mass increase from C to Si cannot explain the observed effect.

Instead, we have found that a far more important feature responsible for the anomalous lifetime of the CH vibration in the Si compound is connected with a bottleneck in relaxation pathways. The bottleneck substantially decreases the cumulative transition amplitude from the initial state and virtually results in vibrational energy localization.

Two opposite models of vibrational coupling in large molecules can be envisaged. In one limiting model the high order anharmonic couplings would be assumed to be equally important as the low order ones. That is, all zeroth-order harmonic states could be coupled directly independently of vibrational numbers of those states. In this model one would expect a strong correlation between the IVR rates and the total densities of states, since all states can be directly reached by the anharmonic couplings.

In an alternative limiting model it would be assumed that the higher order couplings are, instead, mainly due to the high order perturbation theory interactions, arising from a sequential effect of low order anharmonicities, i.e., proceeding via many virtual transitions. The direct high order anharmonicity couplings are assumed to be less important than the sequential ones. For example, two states differing in six vibrational quantum numbers can be coupled by the sixth-order anharmonicities with first-order perturbation theory, or, instead, with cubic couplings using second-order perturbation theory. With the latter type of couplings all states still can be mixed sequentially in a higher order perturbation theory. The importance of the total density of states is then less obvious. A key question concerns the relative importance of these direct and indirect couplings.

In this paper we study a model of IVR based on cubic and quartic anharmonic couplings. The nature of the coupling in this model makes the total density of states, as noted earlier, less relevant than the details of the coupling, as far as relaxation dynamics of the initially prepared state and, hence, to the spectral broadening of the state are concerned. An assumption of low order couplings results in a quantum mechanical model in which all quantum states are grouped in sequentially coupled tiers. Levels from the first tier are directly coupled to the initially prepared state, the latter have been prepared through a radiative transition from the ground vibrational state, and is also coupled to the states in the second tier. The second tier, in turn, is coupled to third tier, etc. This model is referred to as a tier model.[10,20,21]

The number of states effectively coupled to the initially prepared state, and the cumulative density of states, increases rapidly with the number of tiers taken into account. For relaxation to occur the density of coupled states should be high enough to ensure the statistical limit. The average effective coupling of the initial state to levels in the nth tier is of the nth order. When the coupling between tiers is weak, this effective interaction is an exponentially decreasing function of n. In the weak coupling case it might happen that the effective interaction decreases faster than the increase of the density of states. The statistical limit will then not be reached even when all states are included. In this situation localization of vibrational energy occurs. The localization means essentially that the initial state is effectively mixed with only a few states, at best, instead of being strongly mixed with almost all states of the same energy.

An example of such a situation, namely Anderson (quantum) localization, is well known in the solid state physics, as in Refs. 35 and 36. Since the tier model of IVR resembles in many respects the electronic coupling scheme in a random solid, similar phenomena should be expected in both cases. The localization phenomenon has been recently discussed in a context of IVR by Logan and Wolynes.[37]

When the localization occurs only a finite number of zeroth-order states contribute significantly to the eigenstates of the diagonalized system. In this case, instead of an exponential decay of the initially prepared state, at best quantum beats would be expected in the dynamics of that state. The absorption spectrum will contain only one or a few sharp lines instead of the Lorentzian-like contour that would occur when all states are mixed. Our calculations indicate that for the Si compound the dynamics of the CH vibration resembles the localization described earlier.

We discuss also the computational details. It has been found that C programming, in connection with highly optimized FORTRAN routines, provides a powerful tool to study pathways of vibrational relaxation in large molecules. Different methods have been tested, including a modified recursive residue generation method (RRGM) of Wyatt[3] in which the calculation of overtone spectra does not require any diagonalization at all. In this method systems including as many as 30 000 states were studied.

The structure of the paper is as follows. In Sec. II some

theoretical aspects of the tier model are discussed. In Sec. III the construction of the model potential field of the molecules is outlined, and in Sec. IV theoretical methods used in the paper are briefly described. The results are discussed in Sec. V.

II. TIER MODEL

In this section the main approximation for a vibrational Hamiltonian of large molecules which results in a tier model is discussed. We consider a molecule in the ground electronic state and consider only the vibrational intramolecular interactions. Although IVR mediated by vibration-rotation interactions has been shown to play an important role in specific situations, e.g., in Refs. 38 and 39, we concentrate, in the present article, on the case where the vibrational interactions are dominant.

Before discussing a multitier model it is useful to recall a general model which has been adapted to IVR problem[40] and to overtone spectroscopy. It consists of a "light" state coupled to a one-tier manifold of background "dark" states, $\{|l\rangle\}$. The light state, directly accessible in an overtone transition, is not an eigenstate of the molecule and, hence, is subject to a time evolution in which it mixes with the background states. The theory for this model predicts that if the density of background states, ρ, is high enough and coupling is strong, the initially prepared state will decay exponentially[40] and its decay rate constant Γ can be calculated by the Golden Rule,

$$\Gamma = 2\pi |M|^2 \rho_v , \tag{2.1}$$

where the density of states ρ_v is the total density of vibrational states at the energy of the light state, and M is the effective average coupling matrix element, defined later. It is presumed that the background states are prediagonalized states for the whole system, apart from the light state. Depending on a parameter κ,

$$\kappa = |M| \rho_v , \tag{2.2}$$

the time evolution of the light state can vary from this pure exponential decay, when κ is large, with a decay constant given by Eq. (2.1), to an essentially localized behavior with no energy transfer at all, when κ is small. For the intermediate values of κ quantum beats in the time evolution of the initial states would be predicted.[40] In this manner, for any given ρ_v, M defines the dynamics of the initial state. The problem, hence, is to calculate M by prediagonalizing all relevant states.

A general model of sequentially coupled vibrational states in polyatomic molecules has been discussed in the literature in the past, for example in Refs. 10, 20, and 21. The theory is based on the assumption that the anharmonic interactions of the lower orders are the ones of principal importance in the Hamiltonian. High order interactions between zeroth-order states then arise in high orders of perturbation theory.

The Hamiltonian in the present paper is assumed to be known in normal mode coordinates up to the fourth order in anharmonicity,

$$H = \sum_{i=1}^{s} \omega_{0i} \left(\frac{P_i^2}{2} + \frac{Q_i^2}{2} \right) + \frac{1}{3!} \sum \Phi_{ijk} Q_i Q_j Q_k + \frac{1}{4!} \sum \Phi_{ijkl} Q_i Q_j Q_k Q_l . \tag{2.3}$$

The zeroth-order states are taken to be harmonic ones $|v_1 \ldots v_s\rangle$. Their energies, however, are calculated according to an expression which takes into account first-order intramode anharmonic corrections,

$$E(v_1,\ldots,v_s) = \sum_{i}^{s} \omega_{0i}(v_i + 1/2) + \sum_{i}^{s} x_{ii}(v_i + 1/2)^2 \tag{2.4}$$

with spectroscopic constants x_{ii}. (The *intermode* anharmonicities x_{ij} were not taken into account in the present calculations.) In calculating the cubic and quartic coupling matrix elements between modes, on the other hand, the wave functions used were the unperturbed harmonic oscillator ones. These matrix elements can be calculated from the harmonic oscillator rules and do not require numerical integration. As a perturbation between zeroth-order states we then include only anharmonic terms of the potential energy which do not contribute to the $E(v_1,\ldots,v_s)$ in Eq. (2.4) but which contribute to the mixing of quasiresonant zeroth-order states. Anharmonic terms which contribute to Eq. (2.4) can be represented as Morse oscillator terms in the individual normal modes, without cross-terms.

Anharmonic cubic interactions in second-order perturbation theory couple states which could also be directly coupled by the quartic anharmonicity; in a similar way the third-order couplings could be reproduced by direct quintic coupling, etc. Thus, in principle, the cubic terms alone may lead to inclusion of all states in the system. However, such an approach based only on cubic terms would be valid only when the average occupation number in each of the vibrational modes is low. This situation is not the case for all vibrational states at a given energy. For example, when the entire energy of the acetylenic CH excitation becomes concentrated in a low frequency vibrational mode the occupation number in the latter can be very large. In this case anharmonicities higher than cubic and quartic would be required to describe the potential energy function correctly. However, the statistical weight of such states is very small and for the vast majority of states the Hamiltonian (2.3) is expected to be a reasonable approximation.

We let the light state in a spectroscopic experiment correspond to a vibrational excitation in mode 1. For molecules of interest in the present paper these states correspond to the excitation of the acetylenic CH bond. Thus, the zeroth-order state $|v,0,\ldots\rangle$, where v is the excitation number, can be accessed directly via a radiative transition. This state is coupled to quasiresonant vibrational states in which the excitation energy is distributed among different vibrational modes of the molecule, modes other than mode 1. Cubic and quartic anharmonicity can couple directly only those states which differ in three and four quantum numbers, respectively. Most of the states will be coupled indirectly in high order perturbation theory. In order to distinguish between direct and indirect couplings all states

are sorted in tiers T_0, T_1,... . States belonging to nth tier can be coupled only to states from T_{n-1} or T_{n+1} tiers by cubic anharmonicities, while quartic interactions will mix states from n and $n\pm 2$ tiers. We separate states coupled by cubic and quartic interaction in different tiers in order to study their relative importance.

Specifically, the states are placed in tiers according the following recursive procedure. The initial light state belongs to tier T_0. Given all the states in tiers T_0,...,T_n, states in T_{n+1} can be generated by applying the cubic anharmonicity operator,

$$V^{(3)}=\frac{1}{3!}\sum \Phi_{pqr}Q_pQ_qQ_r \tag{2.5}$$

to the states in T_n. This operation can produce not only states in T_{n+1} but also states in a previous tier T_{n-1}. The next step is to eliminate any states which belongs to the previous tier. Formally, this operation can be described as follows. Let P_n be the projection operator on the subspace of the tier T_n. It can be written as

$$P_n=\sum_i |n,i\rangle\langle i,n|, \tag{2.6}$$

where $|n,i\rangle$ is the normalized ith state in tier T_n. The normalized jth state in T_{n+1} is then defined by the equation

$$|n+1,j\rangle=(1-P_{n-1})\Omega^{\pm}_{pqr}|n,i\rangle, \tag{2.7}$$

where the Ω operator is defined with harmonic creation and anihilation operators, a^+ and a, for different vibrational modes in the molecule,

$$\Omega^{+}_{pqr}=\frac{a_p^+a_q^+a_r}{[(v_p+1)(v_q+1)v_r]^{1/2}}, \tag{2.8a}$$

$$\Omega^{-}_{pqr}=\frac{a_pa_qa_r^+}{[v_pv_q(v_r+1)]^{1/2}}. \tag{2.8b}$$

The creation and anihilation operators change the occupation vibrational number in a mode by ± 1. Starting from the initial state of T_0 all other states can be generated by applying Eq. (2.7) recursively with all possible indices pqr. To generate $|n+1,j\rangle$ state with approximately the same energy as that of $|n,i\rangle$, only resonance anharmonic terms need be employed in Eq. (2.7). For such terms vibrational frequencies ω_p, ω_q, and ω_r are in resonance, within a certain possible detuning described later,

$$\omega_r\approx\omega_p+\omega_q \tag{2.9}$$

and, hence, r, p, and q are unequal. In this selection procedure only states which are directly coupled by an approximate resonance [in practice the detuning in Eq. (2.9) is of the order of 100 cm^{-1} or less] are considered. There are, however, quasiresonant states which are coupled indirectly through one or more significantly off-resonance states. Such states, which are at least four tiers away, can be created by applying operators $(a_p)^3$ or $(a_p^+)^3$ and then operators (2.8). The intermediate state in this case has a large detuning $3\omega_p$, which is typically of the order of 1000 cm^{-1}. Thus, two states wich are four tiers away can be coupled by a second order with one well off-resonance state, or by the fourth order coupling with three intermediate states which have much smaller detunings, as in Eqs. (2.7)–(2.9). In the procedure described by Eqs. (2.7)–(2.9) it is assumed that contribution of the couplings of the former type is negligible.

Thus, all states are classified according to the order of coupling to the light state rather than according to the number of vibrational quanta, as in Ref. 1. According to the procedure described earlier, the first tier, T_1, will contain states with two vibrational quanta directly coupled to the light state, the second tier, T_2, will contain states with three quanta, or with one quantum, because of the action of Ω^- operator which anihilates two quanta and creates only one, etc. Thus the nth tier will contain states with $n+1$, $n-1$, $n-2$,... states. The projection operator P in Eq. (2.7), applied to *all* tiers recursively starting from the first one, makes sure that among the states with say k quanta in the $n+1$th tier T_{n+1} there would be no states identical to the previously accounted ones also containing k quanta. To exclude the appearance of the same state in different tiers in a recursive procedure it is sufficient to check only the previous tier, T_{n-1}, as in Eq. (2.7). All other tiers are then automatically checked in the previous steps of the recursive procedure.

The procedure described above is readily implemented on a computer. A similar procedure was discussed earlier in a different context.[41] For some molecules of present interest, $(CH_3)_3CCCH$ and $(CH_3)_3SiCCH$, the first few tiers are shown in Fig. 1.

An important characteristic of the tier model is the density of states in tiers, η_n. The densities in the tiers as well as the total number of tiers depend on the energy of a molecule. In the following analysis the accumulated densities will also be of interest:

$$\rho_n=\sum_{m=1}^{n}\eta_m. \tag{2.10}$$

The total vibrational density, $\rho_v=\rho_N$, where N is the total number of tiers. The partial densities (2.10) correspond to the approximate diagonalization of the system in which only first $n<N$ tiers are included.

The background dark states, $\{|l\rangle\}$, introduced in the beginning of this section, can now be specified as the eigenstates arising from the diagonalization of the first N tiers, T_1,...,T_N. The effective coupling of the initial state to a prediagonalized state, l, can be formally expressed as

$$M_{0l}=\sum_i M^{01}_{0i}\langle 1,i|l\rangle+\sum_j M^{02}_{0j}\langle 2,j|l\rangle, \tag{2.11}$$

where

$$M^{01}_{0i}=\langle 0|V^{(3)}|1,i\rangle, M^{02}_{0j}=\langle 0|V^{(4)}|2,j\rangle \tag{2.12}$$

and $V^{(3)}$, $V^{(4)}$ are the cubic and quartic anharmonic terms in Eq. (2.3), respectively. Summation in Eq. (2.11) is over all states i in the first and over j in the second tiers, respectively, M^{01}_{1i} and M^{02}_{1j} are the matrix elements of the states directly coupled to the light state in the first two tiers, and

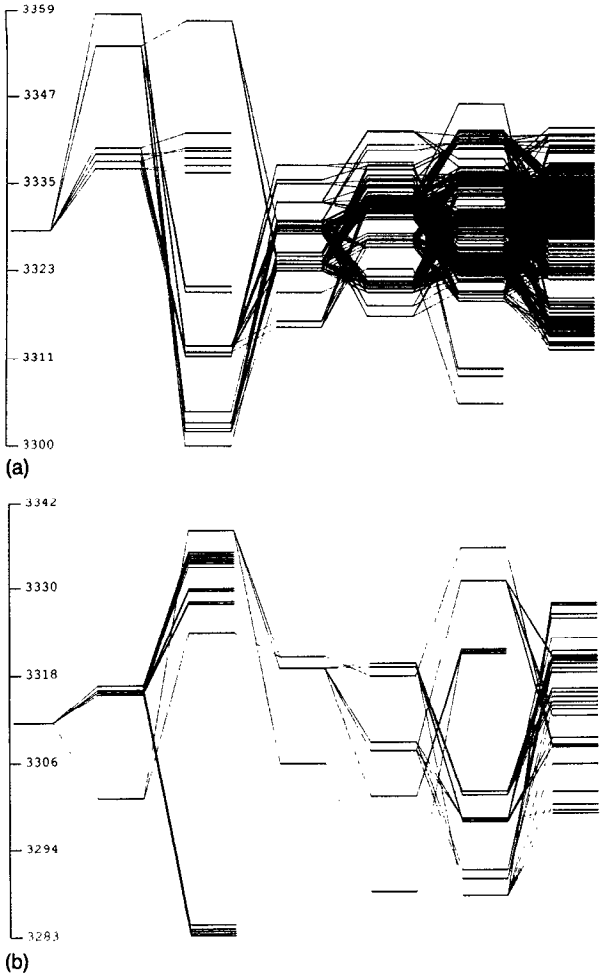

FIG. 1. First six tiers of sequentially coupled zero-order states in (a) $(CH_3)_3CCCH$ and in (b) $(CH_3)_3SiCCH$. The first state on the left is the CH vibration, $v=1$.

$\langle l|1,i\rangle$, $\langle l|2,j\rangle$ are the appropriate coefficients of expansion of the prediagonalized state $|l\rangle$ expressed in terms of the zeroth-order states:

$$|l\rangle = \sum_{n,i} \langle n,i|l\rangle\, |n,i\rangle. \tag{2.13}$$

This $|l\rangle$ is an exact background state for N tiers, i.e., an eigenstate of the diagonalized system of $T_1,\ldots,T_N$. The completeness condition for $|l\rangle$ states in Eq. (2.11) results in the sum rule

$$\sum_l |M_{0l}|^2 = \sum_i |M_{0i}^{01}|^2 + \sum_j |M_{0j}^{02}|^2. \tag{2.14}$$

We note for use in Eq. (4.4) here that the right hand side, and hence the left hand side, of Eq. (2.14) is independent of the number of tiers.

If all of the matrix elements in a tier were of the same order, given by the average values $|M^{01}|$ and $|M^{02}|$ for the first two tiers, respectively, and by $|M|$ for the effective matrix element, then the sums in Eq. (2.14) could be rewritten approximately in the form

$$|M|^2\rho_v \simeq |M^{01}|^2\eta_1 + |M^{02}|^2\eta_2\,. \tag{2.15}$$

From this expression it would be possible to estimate the linewidth, Eq. (2.1), using only the states in the first two tiers. The spectrum of the system restricted to two tiers, however, would look quite different from the actual spectrum because the number of states would be inadequate. A role of the remaining states then would be to provide an appropriate density of spectral lines, while the width itself would be completely defined at the first step of relaxation. Lorentzian broadening of the absorption line can be expected when the effective matrix elements are large enough to satisfy the statistical limit condition,

$$|M|\rho_v \cong (|M^{01}|^2\rho_v\eta_1 + |M^{02}|^2\rho_v\eta_2)^{1/2} > 1. \tag{2.16}$$

Again, to make an estimate of whether or not there will be substantial broadening one seems from Eq. (2.16) to need only the parameters of the first two tiers and the total density of states ρ_v. Those calculations, however, can provide only a very rough estimate of the width. A much more accurate procedure involves similar calculations with a large number of tiers. In this case the couplings and densities are calculated locally, at the quasiresonant position of the light state and on a scale corresponding to observed broadenings, i.e., roughly 1 to 10^{-1} cm^{-1}. In contrast, for the first two tiers the energy window for the calculation can only be of the order of 100 cm^{-1} to have a sufficient number of states for good statistics.

The application of Eqs. (2.15) and (2.16) is limited to a special case of very strong coupling, when all zeroth-order states with the same energy are strongly mixed. It may happen, however, that the matrix elements M_{0l} will vary with l to such an extent that averages $|M^{01}|$ and $|M^{02}|$ in Eqs. (2.15) and (2.16) will be meaningless. In an extreme case the vast majority of the M_{0l} could be essentially zero and the density of spectral peaks would then be much smaller than the total density of states, even if the condition (2.16) were satisfied. This case corresponds to the localization of vibrational energy or, at least, to a significantly restricted IVR.

III. MODEL POTENTIAL SURFACES

The vibrational analysis was performed with a modified version of the quantum chemistry program SPECTRO.[42] To find the anharmonic constants for the Hamiltonian (2.3) the following two-step procedure was used.

In the first step approximate quadratic force fields in internal coordinates for the molecules $(CH_3)_3CCCH$ and $(CH_3)_3SiCCH$ were determined by the procedure of fitting normal modes frequencies of the molecules to the experimental frequencies.[43,44] The equilibrium geometry parameters are known from the electron diffraction data:[45,46] SiC 1.866; SiC≡1.830; C≡C 1.200; CH 1.100; ≡CH 1.077; ∠≡CSiC 107.5; ∠SiCH 112.0. In the calculations C_{3v} symmetry was assumed, as suggested in Ref. 45.

In the second step a nonlinear transformation from internal coordinates to normal modes was used to generate anharmonic constants for the normal modes. Due to the nonlinear character of transformation from internal to normal modes, even a pure harmonic force field in internal

TABLE I. Anharmonic constants in internal coordinates.

(ijk)[a]	f_{ijk}[b]	Reference
$r_1r_1r_1$	−38.0	50
$r_2r_2r_2$	−33.2	48, 52, 51
$R_1R_1R_1$	−50.0	50, 60
$R_2R_2R_2$	−24.5	51
$r_1r_1R_1$	0.4	50
$r_1R_1R_2$	−0.012	50
$r_1R_1R_1$	−0.193	50
$r_1\alpha\alpha$	−0.202	50
$R_1\alpha\alpha$	−0.802	50
$R_1\alpha\beta$	0.346	50

[a]Notation: r_1(≡CH); r_2(—CH); R_1(C≡C); R_2(C–C,C–Si); α(∠HC≡C); β(∠C≡CC).
[b]Units for anharmonic constants consistent with energy measured in aJ, stretching coordinates in angstroms, and bending coordinates in radians.

coordinates contains anharmonic corrections in the cartesian normal modes. These corrections arise from the kinetic couplings. The transformation matrix for anharmonic constants in internal and cartesian normal modes is known in a general form[47] and the procedure is implemented in the computer program SPECTRO.[42] This program was used in the calculation of the quadratic force field and the anharmonic potential energy terms containing cubic and quartic constants.

In addition to pure kinetic couplings the most essential anharmonic potential energy couplings were taken into account. In the calculation we used curvilinear cubic anharmonic constants based on values known for smaller molecules containing the same functional groups. Available cubic anharmonic constants for C_2H_2, CH_3Y, Y=Br, I, Cl, $(CX_3)CCH$, X=F, H, C_2H_6 were analyzed to find reasonable approximations for the present calculations. For the methyl groups a local mode model developed for $(CH_3)X$ molecules[48,49] was used. It was thus possible to describe rather completely, but in an approximate way, anharmonicities of the methyl groups, the anharmonicities of the stretches of all CC and CH bonds and some bond-angle anharmonicities. The set of cubic anharmonic constants used in the calculations is given in Table I. On the other hand, anharmonicities of interaction between the methyl groups were not explicitly included, nor were the other anharmonic constants related to hindered rotation of these methyls.

It should be stressed, of course, that these constants are only rough approximation to the actual anharmonicities of the real molecules. Only those constants were used which were available in the literature from *ab initio* calculations or from other sources for similar molecules, and the assumption was made that those constants are transferable from one molecule to another. The idea of transferability of anharmonic constants has been tested and discussed in recent *ab initio* calculations of small molecules.[50–52] Although this transferability is not exact and can vary from one molecule to another, this procedure seems to be the only way of constructing an at least qualitatively correct anharmonic field at present, in the absence of detailed calculations for these molecules. Because of the large number of degrees of freedom the tables of anharmonic constants in normal modes are extremely large and are only available in a form of computer files.

TABLE II. Anharmonicity factors and spectroscopic constants. Spectroscopic constants x_{ii} were calculated from the anharmonicity factors x_i of Ref. 53 for methyl acetylene.

Type	x_i	x_{ii} (d_i)[a]
CH_3 (*st*)	0.040	0.02(1),0.013(2)
CH_3 (b)	0.020	0.01(1),0.007(2)
CC (*st*) (b)	0.015	0.008(1),0.005(2)

[a]Shown in parentheses is a degeneracy of vibrational mode, d_i.

In the calculations of the zeroth-order energy levels given by Eq. (2.4), typical approximate values of spectroscopic constants x_{ii} were used for different groups of vibrations. The constants x_{ii} were calculated from the anharmonicity parameters of Duncan *et al.*[53] for methyl acetylene,

$$d_i x_{ii} = x_i = (\omega_i - \nu_i)/\omega_i , \tag{3.1}$$

where ω is the harmonic frequency, ν is the fundamental transition frequency, d_i is the degeneracy of the ith vibrational mode, and x_i is defined in the second equality (3.1). The parameter x_i depends only on the type of vibration, as in Table II, but the spectroscopic constants x_{ii} depend also on the degeneracy of a mode d_i. Generally, each vibrational mode was associated with a particular group in the molecule and a particular type of motion. Typical values of x_{ii} were then taken for the same type of motion and for the same group. For example, we distinguished between the CH vibrations and the CC vibrations, between bond stretches and bendings, but, we did not distinguish between different CC bonds, as in Table II. For the vibration of the acetylenic CH the data of Refs. 1 and 2 were used.

The potential surface with cubic and quartic anharmonicities was developed in this manner. As noted earlier, in this approach the internal rotations of the methyl groups were not described, but rather were treated as anharmonic oscillators. Intramolecular rotations is a significant feature of the $(CX_3)_3YCCH$ molecules, which requires a more complicated treatment. Such a treatment we plan to describe in a future publication.

IV. METHOD OF CALCULATION

A. Zeroth-order system

The zeroth-order system is constructed in the first step of the calculation. The problem here is to select from all the states only main ones that affect the relaxation dynamics.

In a detailed description of vibrational couplings in the system each vibrational state is characterized by 42 vibrational quantum numbers, a zeroth-order vibrational energy which is defined by Eq. (2.4), the number of the tier to which the state belongs, the number of states coupled to this particular state in the next tier, a specification of the quantum states which are coupled to this state in the next tier, the matrix elements of this coupling, and some other parameters discussed below. In our computer codes the

linked lists of the data structures of the C language are used to keep account of all this information. The description of this technique is given in textbooks on C, such as Ref. 54. Each level is characterized by a data structure containing different types of information: integer vibrational quantum numbers, floating point matrix elements and energies, complex Green functions, pointers (a pointer being an address in computer memory to a block of data), and some other data referring to the level. In particular, pointers to levels connected to a given state are used to assign appropriate couplings. All data structures are then linked by pointers into a structure representing a blueprint of vibrational couplings in a molecule.

Thus, in the first step the structure of coupled zeroth-order states is generated. The criterion of acceptance of a level in this structure is based on a perturbation theory expression for the effective matrix element. Namely, each of the levels $|i\rangle$ is characterized by a parameter ξ_i

$$\xi_i = \prod_{j=1}^{i} \left| \frac{V_{j-1,j}}{(E_0 - E_j)} \right| \tag{4.1}$$

where j denotes the jth state along the quantum path from the light state $|0\rangle$ to $|i\rangle$. If the energy denominator $(E_0 - E_i)$ for a particular state is too small, so that ξ_i parameter is larger than unity, then the ξ_i for this state is replaced by unity. (Subsequent states along that path then have as ξ a product only of the subsequent factors, $\prod_j |V_{j-1,j}/(E_0 - E_j)|$). A lower limit of acceptance for all states was set equal to some value ξ^L, and then only states with $\xi \geqslant \xi^L$ were accepted in the search. The parameter ξ^L was varied in the range 0.1–1.0, apart from the parameter for the first two tiers. Because of the relatively small coupling of the CH vibration to the rest of the molecule, a substantially weaker criterion was used to form the first two tiers. All states in those tiers were assigned the parameter $\xi = 1.0$ and then the rest of the system was generated according to the procedure described earlier.

Finally, to generate all possible candidates for states in the next tier, in the procedure described by Eqs. (2.6)–(2.8) a list of third-order resonances allowed by symmetry,

$$\omega_i \approx \omega_j \pm \omega_k , \tag{4.2}$$

was used, where ω_j denotes the vibrational frequency of mode j, instead of a direct counting of states with all possible quantum numbers. States which are sufficiently detuned from such a resonance will have a large denominator in Eq. (4.2) and, hence, have a small cumulative value ξ, Eq. (4.1), and so make little contribution. Because of the large number of degrees of freedom, 42, a direct brute force selection process with a systematic overcounting of all quantum numbers is extremely inefficient. On the other hand, the number of the third-order strongly coupled resonances allowed by symmetry, even with a detuning of 500 cm^{-1} from the resonance condition (4.2), is typically only of the order of 100 to 500. Searching the list of such resonances is much faster than the direct counting and one can generate directly, within some reasonable window, states already selected by symmetry. Again, during the selection of resonances only resonances with significant anharmonic constants were taken into account. Examples of zeroth-order states sequentially coupled in tiers are discussed in the next section. Once the structure of the zeroth-order coupled states is obtained various questions about the system can be addressed.

B. Application of the sum rule

As discussed in Sec. II, a sum rule can be used to calculate the spectral width. However, an estimate based only on the first two tiers is not accurate, because of fluctuations of matrix elements and inadequate statistics. Instead of using the first two tiers in the calculations of the width, a sufficiently large number of tiers, $n \sim 10$, was prediagonalized to determine the appropriate background eigenstates. Effective couplings to those states, M_{0l}, were calculated according to Eq. (2.11). Then, a formal application of the Golden Rule yields

$$\gamma_{GR} = 2\pi \frac{\Sigma |M_{0l}|^2}{\delta} = 2\pi \frac{\Sigma |M_{0l}|^2}{K} \frac{K}{\delta}$$

$$= 2\pi \langle |M_{0l}|^2 \rangle \rho_n , \tag{4.3}$$

where the sum is over eigenvalues l in an energy range δ, K is the number of these background states in the energy window δ, $\langle |M_{0l}|^2 \rangle$ is defined by the last equation, and ρ_n is the cumulative density of the background states. To give a correct estimate, δ in Eq. (4.3) should be small enough to provide local information about the couplings in the immediate vicinity of the resonance with a light state, and large enough to contain many states for good statistics. In our calculations δ's of the order of 1 cm^{-1} were used, while the calculated width was in the range 10^{-1} to 10^{-2} cm^{-1}, and the number of states within the window δ was $K \sim 20$–50. It should be noted that even in this case the calculation is only meaningful if it is insensitive to changing the energy window δ around the chosen small value of 1 cm^{-1}.

If $|M_{0l}| \ll \delta$ then the width γ calculated with Eq. (4.3) will not depend on n, the number of tiers used, because of the sum rule. If there is a strong mixing in the system and if the line shape is Lorentzian when all states are taken into account and the density of states is high enough, the Golden Rule can predict the width without diagonalization of the entire system. However, in the case when there is insufficient mixing in the system, the Golden Rule width γ_{GR} will be inapplicable to the spectrum. For example, the absorption spectrum may consist of only a few lines instead of smooth Lorentzian contour. In this case only a few matrix elements will be substantially large, while the vast majority of the matrix elements will be virtually zero.

To check if the additional tiers result in a higher mixing in the system, we calculated in addition to γ_{GR} the average matrix element $\langle |M_{0l}| \rangle = \Sigma_l |M_{0l}/K|$ and examined how it behaves with increase of n.

In the case of strong mixing one should expect from the sum rule

$$\langle |M_{0l}| \rangle^2 \sim \langle |M_{0l}|^2 \rangle = \frac{\Sigma_l |M_{0l}|^2}{K} = \frac{\text{const}}{K} , \tag{4.4}$$

where the last equality follows from the statement after Eq. (2.14), and, hence, the average matrix element, $\langle|M_{0l}|\rangle$, should behave as

$$\langle|M_{0l}|\rangle \sim \frac{\text{const}^{1/2}}{K^{1/2}}. \tag{4.5}$$

If there were no mixing the decrease of $\langle|M_{0l}|\rangle$ would be expected to be much faster ($\sim 1/K$), because the number of nonzero matrix elements would be essentially unchanged with an increase of N. Hence, in the strong mixing case, it would be expected that the number

$$\bar{\gamma}=2\pi\langle|M_{0l}|\rangle^2\rho_n \tag{4.6}$$

should be of the same order as γ_{GR} (in the case of Gaussian statistics of the matrix elements, one should expect $\langle|M_{0l}|\rangle^2=2/\pi\ \langle|M_{0l}|^2\rangle$ and, hence, $\bar{\Gamma}\simeq 0.6\Gamma_{GR}$) and that its dependence on the number of tiers n would be weak. On the other hand, for the case when the mixing is restricted for some reason, $\bar{\gamma}$ is expected to be much smaller than the actual width γ_{GR} and to decrease with increasing number of states.

In the present calculations the systems are prediagonalized for various numbers of tiers and the behavior of both γ_{GR} and $\bar{\gamma}$ is studied.

C. Calculation of the line shape

It is straightforward to generate the Hamiltonian matrix and to diagonalize it once the the zeroth order structure is given. For relatively large systems this problem can be solved by the RRGM method whose application to IVR has been described by Wyatt.[3] This method provides an efficient technique, although it does require a special handling of the computer memory for large systems. In the present calculations in addition to RRGM we have also used the Green function (GF) technique, described below.

In the Green function technique the spectral absorption line shape is calculated as[41]

$$I(\omega)=\frac{1}{\pi}\,\text{Im}G_{00}(\omega), \tag{4.7}$$

$$G_{00}(\omega)=\langle 0|\frac{1}{(\omega+i\epsilon-H)}|0\rangle, \tag{4.8}$$

where ω is the absorption frequency, ϵ is a resolution of the spectral lines, H is the exact Hamiltonian, and $|0\rangle$ is the initial light state. For a number of cases Eq. (4.7) can be calculated exactly.

For a one-tier system, the absorption spectrum is given by (see the Appendix)

$$I(\omega)=\frac{1}{\pi}\,\text{Im}\,\frac{1}{\omega+i\epsilon-E_0-\Sigma_l|M_{0l}|^2/(\omega+i\epsilon-E_l)}. \tag{4.9}$$

The formula can also be used, for example, after a prediagonalization, i.e., when a system consisting of many tiers is reduced to a one-tier system.

For a one-dimensional chain of levels (an n-tier system with only one state per tier, with energies E_i and couplings $M^{i,i\pm1}$) the absorption spectrum can be calculated with the following recursive relation (Appendix)

$$G^{ii}(\omega)=\frac{1}{\omega+i\epsilon-E_i-|M^{i,i+1}|^2G^{i+1,i+1}(\omega)}, \tag{4.10}$$

where for the last state in the system, L,

$$G^{LL}(\omega)=\frac{1}{\omega+i\epsilon-E_L}. \tag{4.11}$$

This case is particularly interesting because in the RRGM procedure,[3] after a number of Lanczos transformations, the original system is reduced to a one-dimensional chain of levels having the corresponding tridiagonal Hamiltonian matrix. Instead of diagonalizing this matrix one can use Eqs. (4.10) and (4.11) directly to calculate the absorption spectrum for a given frequency. The Lanczos transformation can be applied directly to the data structure of zeroth-order states. This procedure is equivalent to keeping an account of only the nonzero matrix elements in the Hamiltonian matrix. Thus, the Lanczos recursive procedure and the application of Eqs. (4.10) and (4.11) provides a modification of RRGM which obviates use of the diagonalization step. An essentially same recursive method, described by Haydock in Ref. 41, was used for calculation of the local density of electronic states in disordered solids.[41] A similar procedure has also been used by Wyatt and coworkers in quantum scattering problem.[55]

Finally, a combination of the two cases described above results in another exactly solvable system. It is a system of N tiers with unlimited number of states in each tier, where each state interacts with an independent subset of levels from the next tier. In this case a generalization of the recursive formula similar to Eqs. (4.10) and (4.11) exists. For each state i from the nth tier the Green function is expressed in terms of the Green functions of coupled states from the next, $(n+1)$, tier, (see the Appendix)

$$G^{nn}_{ii}(\omega)=\frac{1}{\omega+i\epsilon-E^n_i-\Sigma_j|M^{n,n+1}_{i,j}|^2G^{n+1,n+1}_{j,j}(\omega)}, \tag{4.12}$$

where the summation is over all coupled states from the $n+1$ tier. For the states from the final tier in the system, N, one has

$$G^{NN}_{kk}(\omega)=\frac{1}{\omega+i\epsilon-E^N_k} \tag{4.13}$$

Starting from the last tier all the GF can be calculated recursively. The resulting last GF in this calculation will correspond to the initial light state, G_{00}. Then, the absorption spectrum can be calculated using Eq. (4.7). All nondiagonal elements of the GF are exactly zero because of the independence of the relaxation paths in this hypothetical system.

In the system considered earlier, described by Eqs. (4.12) and (4.13), no more than one state is coupled to the same state in the next tier and in this sense there are no

quantum interferences for relaxation paths of different states. The above formula might be used as an approximation to a general N-tier system where there are quantum interferences, i.e., where there can be more than one state coupled to the same state in the next tier. This approximation means that in the calculation of the quantum amplitude of the "light state-light state" transition of the resolvent operator, Eq. (4.8), over all quantum paths the contribution of some quantum paths is neglected. This procedure corresponds to a random phase approximation, which, on the basis of comparison with the exact diagonalization results, provides a good estimate of the linewidth in large systems.

The complex-valued GF of energy levels for a given absorption frequency can be calculated recursively with Eqs. (4.12) and (4.13), starting from the last tier, N. At the nth step of recursion all GF's of states in tiers $k \geqslant N-n$ are known and written in the data structures of each of the levels. Then the next step of recursion is performed with Eq. (4.12). The process is continued until the light state is reached.

V. RESULTS AND DISCUSSION

A. $(CH_3)_3CCCH$ and $(CH_3)_3SiCCH$: $v=1$

All computations were performed on a CRAY-Y/MP with 80 Mb of memory. Our computer program generates recursively all strongly coupled states starting from a given light state. Examples of such sequentially coupled vibrational states for $(CH_3)_3CCCH$ and $(CH_3)_3SiCCH$ molecules, $v=1$, are shown in Fig. 1. Because of the extremely high density of states in higher tiers and the limited resolution of the plot only the first few tiers are shown.

It was found that the data structures, linked lists, and pointers of the C language provide a natural way for a detailed description of vibrational couplings in large molecules, as in Fig. 1. Each state shown in Fig. 1 corresponds to a data structure in the computer memory and the links between states correspond to pointers. The concept and techniques of linked lists and data structures in C language are discussed in detail in Ref. 54. All states in Fig. 1 are numbered, each level is described by 42 vibrational quantum numbers, its energy, its coupling matrix element to a state from the previous tier, the number of states coupled to it in the next tier, and some other characteristics discussed earlier. All relevant information is stored in the data structures (a data structure is a block of data containing different types of information with an address in the computer memory[54]). All states in a tier coupled to the same state are linked into a list and the address of the list is stored in the pointer of the state in the previous tier to which those states are coupled. Each state has a pointer to a list of directly coupled states from the next tier. It can be an empty list if there are no coupled states in a given window. States from the same tier are linked into a larger list to facilitate manipulations with tiers. The main advantage of the data structures is that the all information relevant to a single state is stored in one place and can be manipulated as single unit. The whole tree of coupled

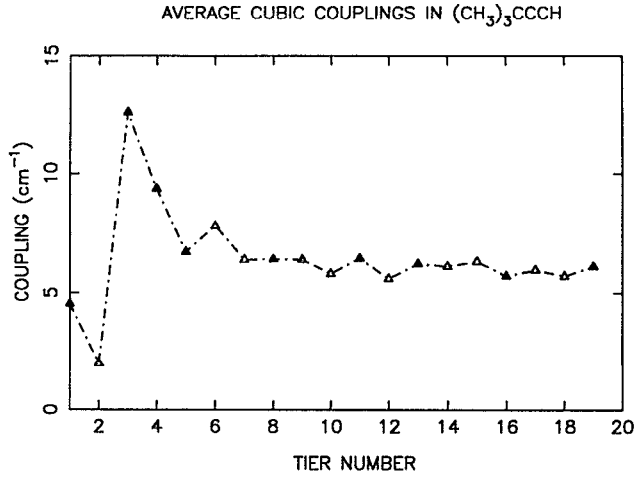

FIG. 2. Average cubic couplings in $(CH_3)_3CCCH$ in different tiers.

structures stored in the computer memory reproduces a blueprint of vibrational couplings in a molecule. Up to 40 tiers and 50 000 coupled states could be generated this way.

The states shown in Fig. 1 provide the first steps of relaxation from the light state. We note that the densities of those states are substantially lower than those required to form broadening on the scale of 10^{-2}–10^{-1} cm^{-1}, as can be seen in the energy scale on Fig. 1. Those states, hence, serve only as a bridge between the light state and the states in higher tiers, where the cumulative density is sufficiently large and where there are many states quasiresonant with the light state in the window of 10^{-2}–10^{-1} cm^{-1}. Those quasiresonant states will form an absorption contour. A correspondence between this type of relaxation and semiclassical dynamics has been recently discussed in context of local modes in symmetric triatomic molecules in Ref. 22. It has been shown[22] that in the semiclassical limit this type of energy transfer corresponds to dynamic tunneling in phase space.[23–27] In a long distance electron transfer reaction this mechanism is also known as superexchange, as in Refs. 56 and 57, for example. This type of coupling for IVR problem can be called a vibrational superexchange.

An example of the dependence of an average coupling matrix element on the tier index n is shown in Fig. 2. A striking and perhaps surprising feature there is that the average coupling does not change very much in the range of 5–19 tiers, as one might have expected from the dependence of the matrix element on vibrational quantum numbers. This fact indicates that even in the higher tiers the average quantum vibrational number in a mode is between zero and one, because of large total number of degrees of freedom. The occurrence of large fluctuations in the first tiers, where the density of levels is relatively low, is due to poor statistics. Although the average coupling of states is less than 10 cm^{-1}, as shown in Fig. 2, there are also couplings in the range 10–30 cm^{-1}. For this reason the energy window for the search of the zeroth-order states cannot be made substantially smaller than that shown in Fig. 1.

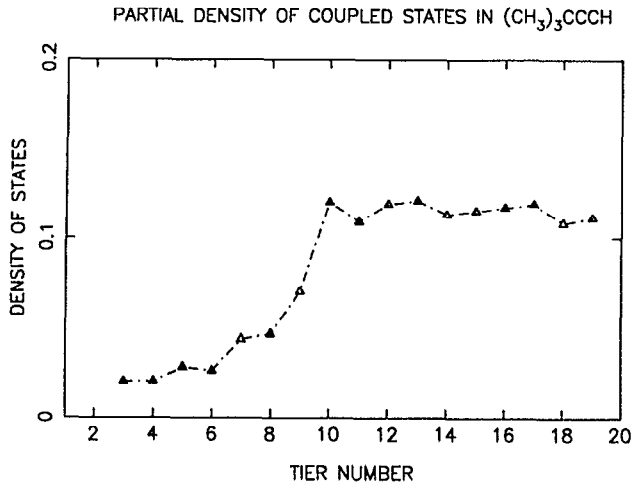

FIG. 3. Partial density of coupled states in $(CH_3)_3CCCH$.

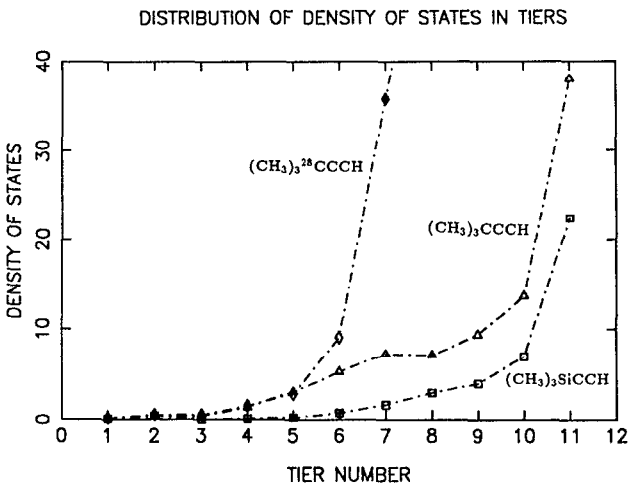

FIG. 4. Distribution of densities of states in $(CH_3)_3CCCH$ (middle curve), $(CH_3)_3SiCCH$ (lower curve), and in $(CH_3)_3\,{}^{28}CCCH$ with a heavy central atom (upper curve). Energy corresponds to CH vibration, $v=1$.

There are, however, also very weakly coupled states, with coupling substantially less than 1 cm^{-1}. Such states can participate in the relaxation dynamics, if they are in good resonance with the light state. The resulting wide range of equally important couplings constitutes the main technical problem in the simulation of such a system. It also results in three orders of magnitude range of different time scales in the system, which yields a substantial numerical problem.

In Fig. 1 a qualitative difference can be seen in the densities of coupled states in the first tiers for the C and Si molecules. Despite the fact that the total density of states in the Si molecule is approximately thirty times higher in this energy region, the local density of directly coupled states in the Si molecule is found to be substantially smaller than in the C molecule, for reasons described later. A particularly low number of strongly coupled states in the tier 3 (the light state is tier zero) of the Si molecule produces a bottleneck for the energy transfer from the acetylenic CH vibrational state. For the C molecule there are already a number of quasi-resonant states in tier 3, as one can see in Fig. 1(a).

A typical behavior of the densities of states directly coupled to a single state (the density per one state) in different tiers for the C molecule is shown in Fig. 3. The density has a tendency to level off in high tiers, which means that the number of different states coupled to the same single state, the branching number, remains more or less the same. The distribution of the total density of states in tiers is shown in Fig. 4. The total density in a tier is less than a sum of densities of states arising from each individual state in the preceding tier, because several states from the previous tier can be coupled to the same state. On the average, typically 2.5 states in a given tier were found in the present calculations to be coupled to the same state in the next tier.

Thus, the density of intermediate states which provide a bridge between the light state and quasiresonant states of higher tiers is larger for a C molecule than for a Si molecule. To address the question of why this behavior occurs, the calculations were made for a model C molecule in which the central atom C has the mass of the Si atom, i.e., $M=28$, while all other parameters of the molecule, including the quadratic force field and the anharmonicities in internal coordinates, remain the same. The results for the densities of coupled states are shown in Fig. 3. The heavy C atom causes two opposite effects. On the one hand, the kinetic coupling between the CH vibration and the tertiary group becomes weaker, due to the heavy atom blocking effect, as discussed in Refs. 28–34. The weaker coupling should result in a lower density of strongly coupled states. On the other hand, due to the same heavy atom effect, the frequencies in the molecule become smaller on the average, an effect which should increase the total density of resonances. This increased total density of resonances is expected to result in a higher density of strongly coupled states. Which factor prevails in $(CH_3)_3CCCH$ molecule is illustrated in Fig. 3. The increased density of resonances clearly prevails over the reduced kinetic coupling in this case.

In the next step of the calculation all states in the system except the light state were prediagonalized and the effective matrix elements between the light state and the eigenstates found in the prediagonalization were calculated according to Eq. (2.11). Then, the local density of states, the average square, and the average absolute value of the matrix elements were calculated for states where energy is in the immediate vicinity of that of the light state. The energy window, δ, for such calculations was varied in the range of 1–5 cm^{-1} to ensure a statistical limit for averages. The Golden Rule width Γ_{GR} was calculated from such data using Eqs. (4.3) and (4.6) as a function of the increasing number of tiers. The results for $(CH_3)_3CCCH$, $(CH_3)_3SiCCH$, and $(CH_3)_3CCCH$ with a heavy central atom, are shown in Figs. 5–8. As is seen there, the width calculated this way, although fluctuating from tier to tier, does not change substantially with the number of tiers. In

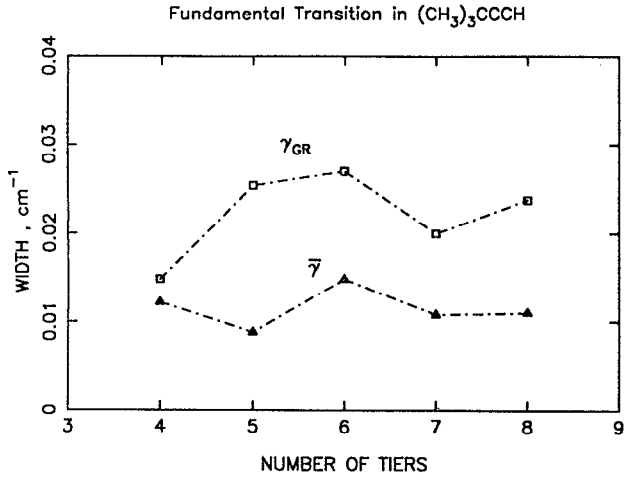

FIG. 5. The Golden Rule width γ_{GR} (upper curve), and the average $\bar{\gamma}$ [Eq. (4.7)] (lower curve) for $(CH_3)_3CCCH$, $v=1$.

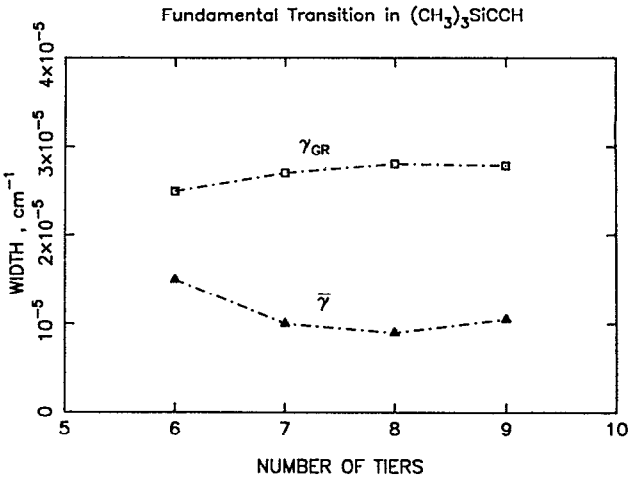

FIG. 7. The same as in Fig. 6, but for cubic anharmonicities only.

all cases the number of states taken into account in the averaging in a small energy window δ varied between 10 and 100. The total number of states diagonalized in this procedure varied between 400 and 2000, depending on number of tiers included in the calculation.

The results for the Golden Rule width calculations, using Eq. (4.3), for different molecules and for the first two vibrational states of the CH vibration, are shown in Table III. An interesting difference between the C and Si molecules was found in the sensitivity of the Golden Rule width to the value of the fourth-order anharmonicities. When all quartic coupling matrix elements were changed from a typical value of the order of 0.05 cm^{-1} to a value of 0.01 cm^{-1}, instead, the Golden Rule width γ_{GR} remained practically unchanged for the C molecule but became 2 orders of magnitude smaller for the Si molecule. This sensitivity in the latter case means that the width in the Si molecule case is mainly due to the fourth-order couplings.

In absence of quartic and higher couplings the Golden Rule width of the Si molecule becomes so small that even for the total density of states it still remains smaller than the average spacings between states. In this situation the vibrational excitation in the acetylenic CH would remain localized, even when all states are taken into account. There might be an accidental degeneracy, in which case a multiplet of lines with splitting less than 10^{-1} might be observed. However, the Lorentzian spectrum would never be formed, no matter how many states were diagonalized. The experimental width, Table III, for the Si molecule is extremely small, of the order of 10^{-3} cm^{-1}, and it does not increase, as it does in a "normal" case of the C molecule, with increase of excitation from fundamental to the first overtone. For such a small width the nature of the broadening is less clear than that of the C case, because of the possible inhomogeneous effects, perhaps accounting for at least a portion of the experimental width in this molecule. In our calculations the CH vibration in the Si molecule is

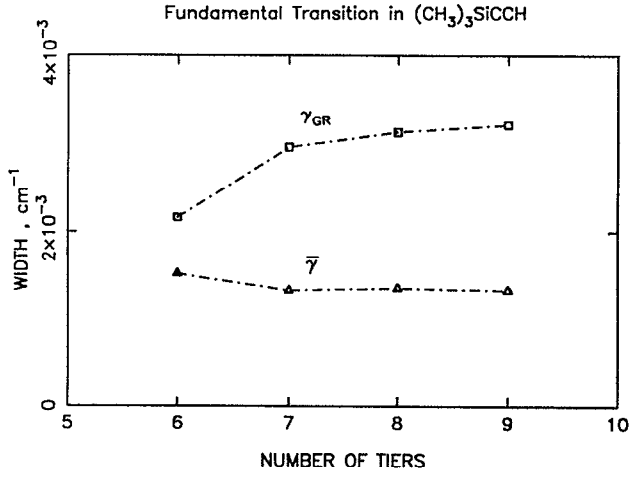

FIG. 6. The Golden Rule width, γ_{GR} (upper curve) and the average $\bar{\gamma}$ [Eq. (4.7)] (lower curve) for $(CH_3)_3SiCCH$, $v=1$.

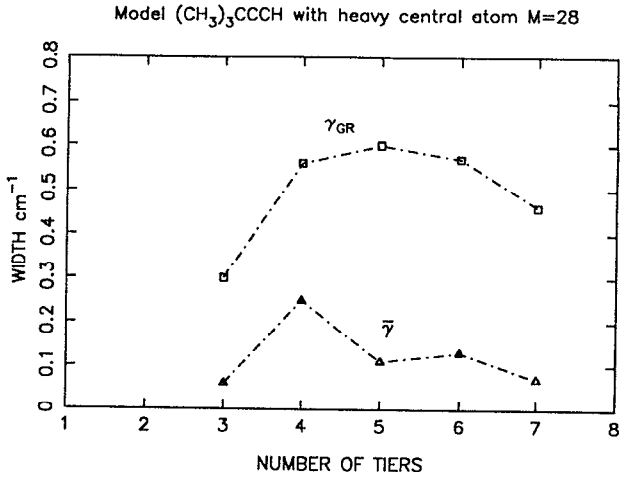

FIG. 8. The same as in Fig. 5, but for $(CH_3)_3CCCH$ with heavy central atom C, $M=28$.

TABLE III. Theoretical Golden Rule widths, γ_{GR}, and experimental widths, full width at half maximum, in cm^{-1}, of acetilenic CH vibration in $(CX_3)_3YCCH$ molecules.

X	Y	v	γ (Exp)	γ_{GR} (Theor)
H	C	1	0.026	0.02
D	C	1	0.13	0.15
H	Si	1	0.0026	>0.0001
D	Si	1	0.0064	0.02
H	C	2	0.048	0.056
D	C	2	>0.25	0.1
H	Si	2	>0.0013	0.004
D	Si	2	0.042	0.03

not broadened at all, on the scale of experimental width 10^{-3} cm^{-1}. Experimental results show, however, that the absorption line for this molecule is undoubtedly homogeneously broadened,[58] but the width is extremely small, as in Table III. Perhaps, the internal rotations, which were not taken into account in our calculation, are responsible for this discrepancy between theory and experimental results.

Calculations of the spectrum itself are much more difficult to perform for these molecules than the width, because in the window of 60 cm^{-1}, which we found to be reasonable for tiers with high numbers, the number of states would be enormous in an exact diagonalization. For example, for the C molecule the density of states should be at least 10^3 per cm^{-1} to reproduce the good Lorentzian observed in the experiment.[2] Hence, the number of states needed to be diagonalized is larger than 60 000. For the spectral calculations the original RRGM method based on the Lanczos recursive transformation,[3] or its modification discussed in the previous section, which does not require diagonalization, can be applied. At the present stage we were able to apply this method for systems with only cubic couplings. In this way systems with as large as 30 000 states could be studied.

We have found that the cubic anharmonicities alone do not produce a dense enough set of spectral lines on the scale of 10^{-2} cm^{-1} to form a smooth envelop for the absorption band observed in the experiments.[1,2] (It should be noted, however, that the experimental spectrum for the C molecule is likely to have some inhomogeneous component which helps to fill in the Lorentzian line shape, without changing its width.[58]) This result means that quartic and perhaps higher anharmonicities are essential for the energy transfer in those molecules. We note that highly anharmonic torsions and rotations, omitted in the present paper, should give rise to anharmonic interactions which may be important in the energy transfer.

However, the exact role of quartic and higher anharmonicities clearly can be different in different molecules. It was mentioned earlier that the Golden Rule width depends significantly on the quartic anharmonicities in the Si molecule, but that results were insensitive to the quartic constants in the C molecule. At the same time the number of spectral lines depends substantially on the presence of quartic anharmonicities in both cases. With quartic couplings the number of states which can be reached directly from a single state is substantially increased and this property seems to be a crucial one for the number of spectral lines in the absorption band.

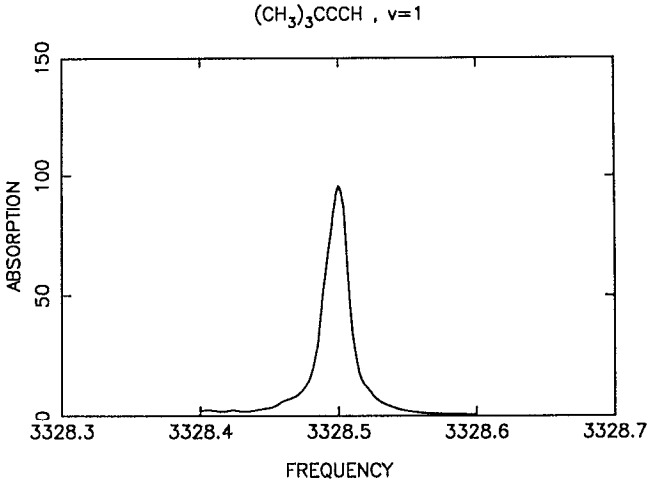

FIG. 9. Calculated fundamental transition in $(CH_3)_3CCCH$.

The general theoretical basis of our calculations is that the width of the absorption band can be calculated from a sufficiently large but limited number of states. To reproduce the line shape of this very highly resolved spectrum, a substantially larger number of states needs to be taken into account. The more states that are taken for diagonalization the closer the spectral absorption line shape should correspond to the exact one.

Additional states are assumed to fill the frequency space between the spectral lines of a smaller system with additional spectral components. One can imitate such an effect to some extent with a low resolution calculation. The resolution, ϵ, should be of the order of spacings between the spectral lines but less than the total width of the absorption band. This kind of calculation for a fundamental transition in $(CH_3)_3CCCH$, $(CH_3)_3SiCCH$, and for

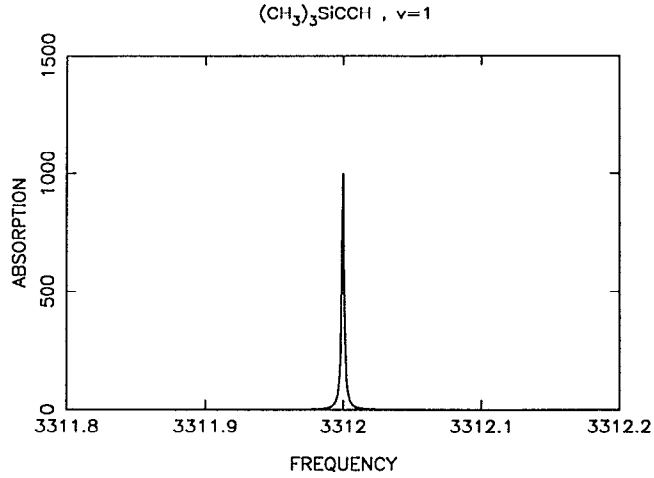

FIG. 10. Calculated fundamental transition in $(CH_3)_3SiCCH$.

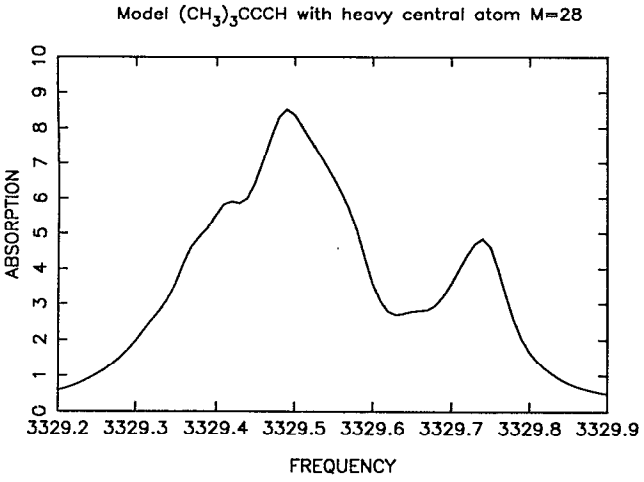

FIG. 11. Calculated fundamental transition in $(CH_3)_3CCCH$ with heavy central atom C, $M=28$.

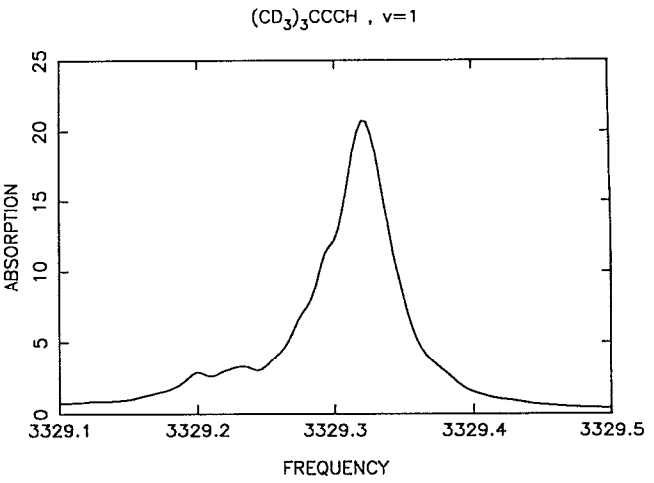

FIG. 13. Calculated fundamental transition in $(CD_3)_3CCCH$.

$(CH_3)_3CCCH$ with a heavy central atom is shown in Figs. 9–11. About 2000 were included in each case. For the Si molecule the spectrum consists of a single line and is not broadened at all. The apparent width in Fig. 10 is due entirely to the low resolution, $\epsilon=0.001\ cm^{-1}$, of the spectrum. An important fact here is that the widths of the spectral bands in Figs. 9–11 (and also in Figs. 12–20 discussed later) are very close to those predicted by the Golden Rule. This result supports the present assumption that when a substantially larger number of states is taken into account the spectral width will remain appropriately the same, while the spectrum will approach the Lorentzian form.

To address, further, the key difference between the C and Si compounds, spectral calculations have also been performed for these two molecules using the same model anharmonic force field. We note that in the previous example of heavy atom substitution the anharmonic constants in internal coordinates were kept the same. However, due to kinetic coupling effects the cartesian coordinates were different. One may ask whether the difference is connected principally with the anharmonic couplings or with the frequencies of vibrational modes. The present calculation can provide an answer to this question. The results are shown in Figs. 12(a) and 12(b), which use

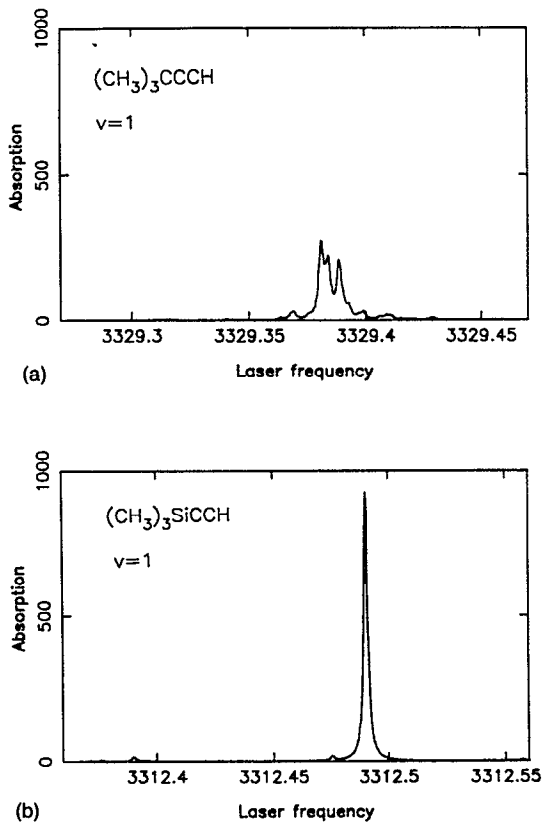

FIG. 12. Calculated fundamental transition in (a) $(CH_3)_3CCCH$ and in (b) $(CH_3)_3SiCCH$ with the same anharmonic field, but differing in the quadratic force field.

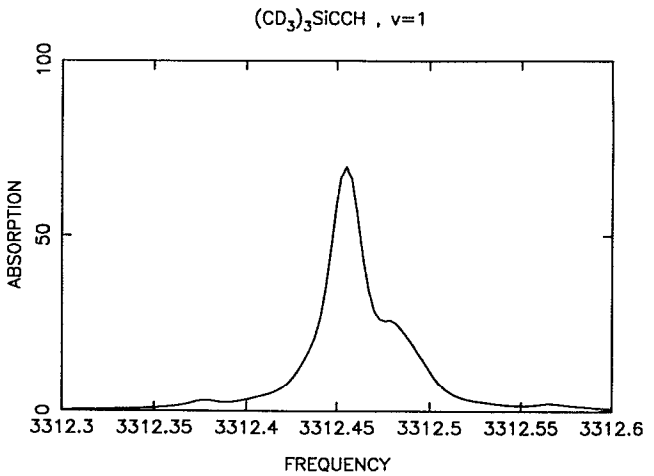

FIG. 14. Calculated fundamental transition in $(CD_3)_3SiCCH$.

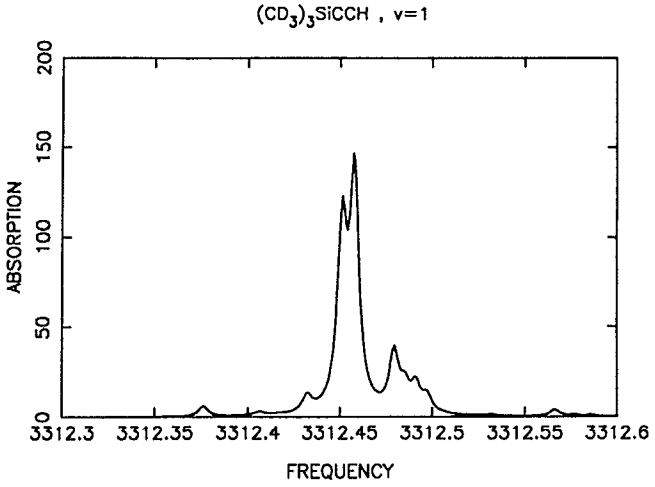

FIG. 15. Calculated fundamental transition in $(CD_3)_3SiCCH$ as in Fig. 14, but with higher resolution.

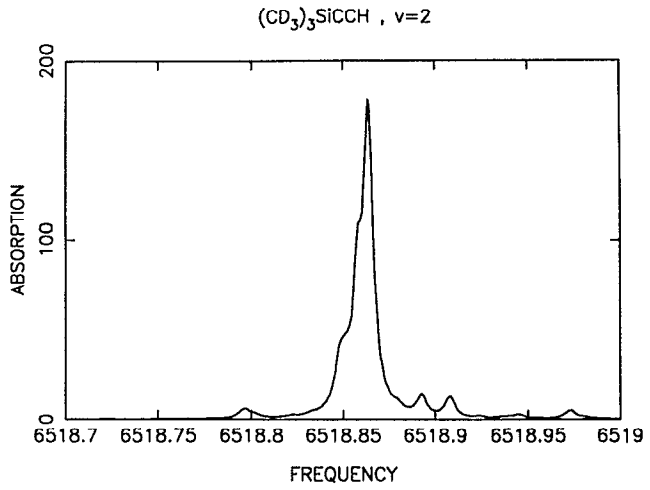

FIG. 17. Calculated first overtone transition in $(CD_3)_3SiCCH$.

the same anharmonicities for the two molecules. About 30 000 states were used in this calculation with the modified RRGM. Although the anharmonic force fields for the two calculations, Figs. 9 and 10 (which have different anharmonicities) and Figs. 12(a) and 12(b) (which do not), were different, the qualitative result is the same: The spectral width in the C molecule is much larger than that in the Si molecule and, hence, the vibrational relaxation from the acetylenic CH mode in the C molecule is substantially faster than in the Si molecule. Therefore, we may conclude that the main difference in relaxation rates for the C and Si molecules is primarily due to different frequencies of the normal modes.

B. $(CD_3)_3CCCH$ and $(CD_3)_3SiCCH$: $v=1$

Results for the fundamental transition in deuterated molecules above are shown in Table III and in Figs. 13 and 14. For both the Y=C and Si cases the deuteration results in substantially larger widths. This observation can be explained by the increased density of resonances due to the lower vibrational frequencies in those molecules. In fact, the same effect was observed for the $(CH_3)_3CCCH$ molecule with the substituted heavy central atom, as in Figs. 9 and 11. Surprisingly good agreement in Table III with the experimental data was obtained for the deuteration effect of the C molecule. The spectral line shapes are not the desired Lorentzians but consist of several peaks, peaks which can be seen in the spectrum with higher resolution, Fig. 15. As in the previous case the calculated width of the low resolution spectral band is in good agreement with the Golden Rule calculations.

C. $(CH_3)_3SiCCH$, $(CD_3)_3SiCCH$, $(CH_3)_3CCCH$, and $(CD_3)_3CCCH$: $v=2$

In the present calculation the first overtone in the $(CH_3)_3SiCCH$ molecules does not show any substantial sign of broadening. Instead, an additional peak, separated

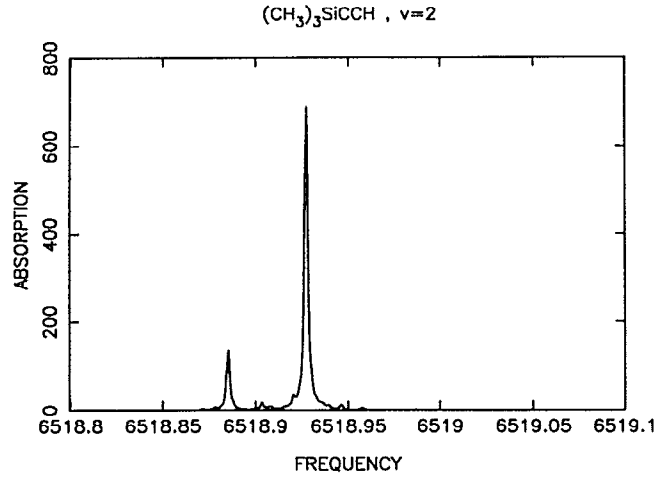

FIG. 16. Calculated first overtone transition in $(CH_3)_3SiCCH$.

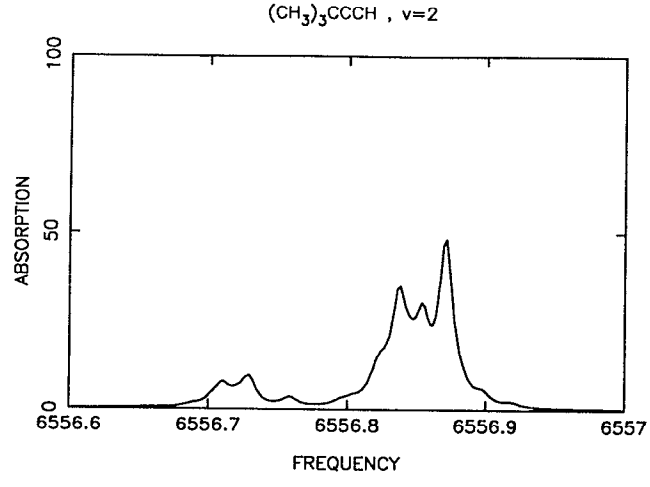

FIG. 18. Calculated first overtone transition in $(CH_3)_3CCCH$.

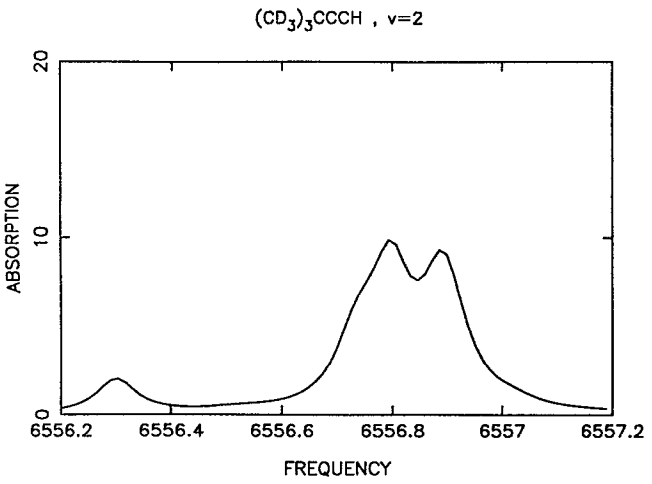

FIG. 19. Calculated first overtone transition in $(CD_3)_3CCCH$.

from the main component by 0.05 cm^{-1}, has appeared in the spectrum, Fig. 16. This peak is clearly due to an accidental resonance of the light state with a state from a distant tier. A total of eight tiers was diagonalized with a total density of states of about 270 states per cm^{-1}. The Golden Rule predicts a width of 0.004 cm^{-1}, as in Table III, which is smaller than the average spacing between the vibrational states at this energy. This result is in agreement with the spectral calculations shown in Fig. 16 which indicate no substantial mixing of the initial state with the background states. The density of states is still not sufficient for the mixing. A surprisingly weak mixing, even for the first overtone in this molecule, is due to the extremely weak interactions of the light state ($v=2$) of the CH vibration with the states in the first two tiers. The average coupling to the first tier was found to be 0.16 cm^{-1}, while the density of directly coupled states was only 0.04 states per cm^{-1}. We have not seen the decrease of the width found on going from $v=1$ to $v=2$ in the experiment of Ref. 1. However, in general, our resolution for spectral calculation is not sufficient to describe what is happening on the scale of 10^{-3} cm^{-1}.

Compared with the X=H case, the average coupling to the first tier in the deuterated molecule $(CD_3)_3SiCCH$ remains approximately the same, 0.19 cm^{-1}, while the density of states in this first tier increases from 0.04 to 0.23 states per cm^{-1}, a substantial increase. The increase is due to the lower frequencies in the deuterated molecule, which provide more low-order resonances. As a result, the Golden Rule predicts a width of 0.03 cm^{-1}, as in Table III, which agrees approximately with the experimental width of the spectral absorption band. The absorption spectrum for $(CD_3)_3SiCCH$ is shown in Fig. 17. A remarkable feature of the experimental spectrum for $v=2$ of the deuterated Si molecule was the presence of two weak but narrow additional features.[58] Although we do not predict these exact features, but it is likely similar to the feature we do predict for $v=2$ of the Si molecule with CH_3 groups, Fig. 16, which arises due to an accidental resonance in an intermediate tier.

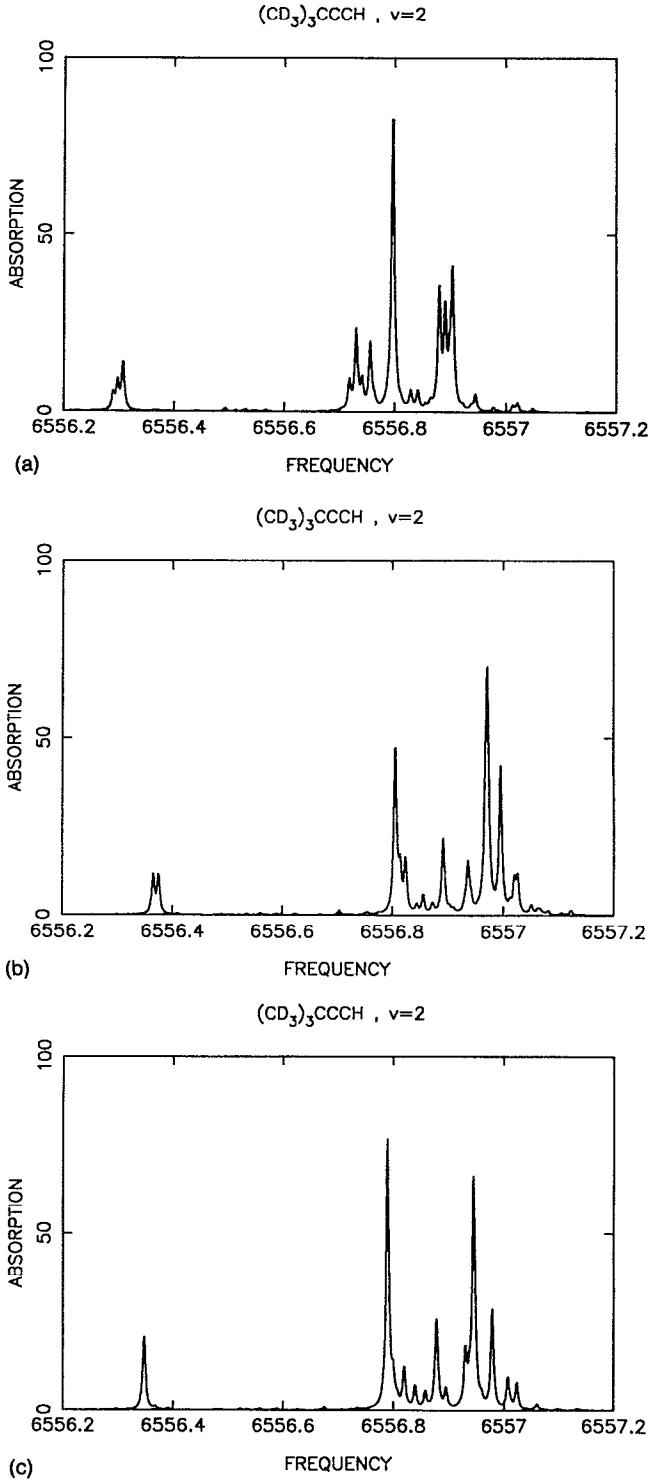

FIG. 20. The same as in Fig. 19, but with higher resolution and for slightly different positions within [(a)–(c)] 0.2 cm^{-1} of the light state CH, $v=2$.

Low resolution spectra of $(CH_3)_3CCCH$ and $(CD_3)_3CCCH$ are shown in Figs. 18 and 19. Corresponding Golden Rule widths are given in Table III. Although the calculated spectra are far from the observed Lorentzian

the spectral widths as well as the Golden Rule width is still in good agreement with the experimental data.

The effect on the spectrum of changing slightly the frequency of the CH vibration is shown in Figs. 20(a)–20(c). It is seen that although the line shape changes as the intensity is redistributed among spectral components, the width of the absorption band practically remains the same.

By the nature of the present calculations, only widths of the absorption bands can be considered as a reliable estimate of the IVR rates. Individual peaks of the absorption bands may have very little to do with the real line shape, when all states are taken into account. Given all the uncertainties in the anharmonic force field it is impossible to predict exact position of individual lines in the spectrum on the scale of 10^{-2}–10^{-1} cm^{-1}. However, it can be hoped that average characteristics, which are only important when many thousands of states contribute to the formation of the spectrum, can be reasonably predicted by the kind of calculations described in the present paper. To understand better a higher resolution behavior and the actually observed Lorentzian nature of the spectral line shape, it will be necessary to include a treatment of the internal rotations of the CH_3 groups, in a way other than the present treatment as anharmonic oscillators.

VI. CONCLUSION

As can be seen in Table III a surprisingly good correlation between the experimental results and the present calculations has been observed in the spectral linewidths for a variety of molecules. This correlation suggests that the bulk part of the estimated anharmonic force field is reasonably close to the reality. Several important questions were addressed within the present model of vibrational mixing in $(CX_3)_3YCCH$ molecules, such as the heavy Y atom effect and the effect of deuteration. However, other questions require additional study. First is the question of the importance of the hindered internal rotations of methyl groups. In our model they were represented by three anharmonic low frequency oscillators. The actual potential surface is more complex than that. Due to strong anharmonicity in this part of the molecule there are probably additional, to what we have accounted for, strong couplings of all zeroth order states in tiers with high numbers. The additional couplings can make the background states after prediagonalization more homogeneously mixed, a consequence which should facilitate the energy transfer from the CH vibration. Second, more accurate and direct *ab initio* calculations of the anharmonic field would be useful for these molecules to test the present model anharmonic force field and to have a more detailed and reliable estimate of the couplings. Although the cubic and quartic interactions seem to be sufficient for rough estimates of the spectral linewidths, the importance of higher order terms for the line shape remains to be investigated. Finally, the mechanism of the relaxation corresponds to a dynamic tunneling.[27] It would be interesting to study quantum and classical correspondence in those molecules and explore this mechanism in a pure dynamical picture. Further work in our group addressing some of the stated questions is in progress.

ACKNOWLEDGMENTS

We wish to thank Professors G. Scoles and K. Lehmann of Princeton University for many helpful and encouraging discussions and for providing us with their experimental results prior to publication, Professor R. E. Wyatt of the University of Texas at Austin for helpful remarks on the manuscript, and Dr. W. H. Green of Exxon Research and Engineering Co. for providing codes of SPECTRO. The assistance of Mr. Aseem Mehta of this Institute in writing software for Fig. 1 is appreciated. We are pleased to acknowledge the financial support of the National Science Foundation. This work is supported in part by the Caltech-JPL CRAY Supercomputing Project.

APPENDIX

In this Appendix the derivation of Eqs. (4.9)–(4.13) is sketched. The general Green function formalism used in the present paper is standard and is described, for example, in Refs. 41 and 59. The Green function of the system (GF) is defined as a matrix element of the resolvent operator. Of special interest for the present problem is $G_{00}(E)$, the matrix element for the light state $|0\rangle$. In terms of this function the overtone spectrum is calculated according to Eq. (4.7). $G_{00}(E)$ is defined as

$$\begin{aligned} G_{00}(E) &= \langle 0|\frac{1}{E-H}|0\rangle \\ &= \langle 0|\frac{1}{E-H_0}+\frac{1}{E-H_0}V\frac{1}{E-H_0} \\ &\quad +\frac{1}{E-H_0}V\frac{1}{E-H_0}V\frac{1}{E-H_0}+\cdots|0\rangle, \end{aligned} \tag{A1}$$

where H is the Hamiltonian of the system, E is a complex energy lying in the upper half of the complex plane E, and $|0\rangle$ is the light zeroth order states of H. The Hamiltonian is divided into a zeroth-order part H_0 and a perturbation V. The main idea is to express the unknown GF, $G_{00}(E)$, in terms of the zeroth-order GF, $G^0_{00}(E)$, defined in a similar way as in Eq. (A1), but with H replaced by H_0 and $V=0$. The general equation for the GF can be written in a Dyson form,[59]

$$\begin{aligned} G_{00}(E) &= G^0_{00}(E)+G^0_{00}(E)\Sigma_{00}(E)G^0_{00}(E) \\ &\quad +G^0_{00}(E)\Sigma_{00}(E)G^0_{00}(E)\Sigma_{00}(E)G^0_{00}(E) \\ &\quad +\cdots=[G^0_{00}(E)]^{-1}-\Sigma_{00}(E)^{-1} \\ &= [E-E_0-\Sigma_{00}(E)]^{-1}, \end{aligned} \tag{A2}$$

where $\Sigma_{00}(E)$ is a so-called self-energy for the state $|0\rangle$. An explicit expression for Σ_{00} in operator form is derived in Ref. 59,

$$\Sigma_{00}(E)=\langle 0|V+VQ\bar{G}QV|0\rangle, \tag{A3}$$

where $Q=1-|0\rangle\langle 0|$ is a projection operator on a subspace which excludes the light state $|0\rangle\langle 0|$, and $\bar{G}$ is a resolvent operator defined in this Q subspace. Using Eq. (A3) one can obtain the exact solutions for several cases discussed later. Those solutions can also be obtained directly from Eqs. (A1) and (A2).

For example, inserting the resolution of the identity, $\Sigma|l\rangle\langle l|=1$, in terms of all zeroth order states in the system in both sides of each V in Eq. (A1), and then using Eq. (A2) as a definition of Σ_{00}, it can be seen that in a one-tier system the self-energy for the light state is

$$\Sigma_{00}(E)=\sum_l \frac{|M_{0l}|^2}{E-E_l} \tag{A4}$$

Equations (A2) and (A4) result in Eq. (4.9). This result also immediately follows from Eq. (A3).

For a system of a one-dimensional chain of levels, $|0\rangle,|1\rangle,\ldots|L\rangle$, with couplings $M^{i,i\pm1}$, the self-energy of the light state, $|0\rangle$, can be obtained in a similar manner. Namely, in Eq. (A1) one again introduces the resolution of identity in both sides of each V. Only terms of the type $\langle i|V|i\pm1\rangle=M^{i,i\pm1}$ are nonzero, and so one finds for the light state

$$\Sigma^{00}(E)=\langle 0|V|1\rangle G^{11}\langle 1|V|0\rangle=|M^{01}|^2G^{11}(E). \tag{A5}$$

Here $G^{11}(E)$ is defined for a system with the $|0\rangle$ state excluded, i.e., for a chain $|1\rangle,|2\rangle,\ldots|L\rangle$. In a similar way, the self-energy for G^{11}, Σ^{11} is expressed in terms of G^{22},

$$\Sigma^{11}(E)=\langle 1|V|2\rangle G^{22}\langle 2|V|1\rangle=|M^{12}|^2G^{22}(E) \tag{A6}$$

which is defined for a system with $|0\rangle$ and $|1\rangle$ states excluded, etc. For the last but one state in the system, $L-1$, the self-energy is expressed in terms of Green function of the last state, L, for a system where all states, except the last one, are excluded. The Green function of a system consisting of only one state is given by the zeroth-order GF,

$$G^{LL}(E)=\langle L|\frac{1}{E-H_0}|L\rangle=\frac{1}{E-E_L} \tag{A7}$$

and

$$\Sigma^{LL}(E)=0. \tag{A8}$$

Making substitution in inverse order one can calculate the GF of the light state. Result of such calculation is given by Eqs. (4.10) and (4.11).

Finally, for a system of N tiers, $T_1,\ldots,T_n$, with unlimited number of states in each tier, where each state interacts with an independent subset of levels from the next tier, an exact solution for GF of the light state also exists. For each state i from the nth tier the self-energy is expressed in terms of the Green functions of coupled states from the next, $(n+1)$, tier,

$$\Sigma_{ii}^{nn}(E)=\sum_j |M_{ij}^{n,n+1}|^2G_{j,j}^{n+1,n+1}(E), \tag{A9}$$

where the summation is over all coupled states from the $n+1$ tier. In a similar way as in the previous case of one-dimensional chain, the GF $G_{j,j}^{n+1,n+1}(E)$ is defined for a system where all states from the previous tiers T_0, $T_1,\ldots,T_n$ are excluded. Green functions of the last tier, T_N, are known exactly, because they coincide with the zeroth-order functions, $G_{ii}^{NN(0)}(E)$, and given by Eq. (4.13). Again, making substitutions in reverse order, one arrives at Eq. (4.12).

The structure of the GF in the last two examples is that of a continued fraction. The number of sequential denominators in such an expression can be very large for realistic systems containing hundreds of thousands of quantum states. To write down an explicit analytic expression for GF in such a case would be very difficult. However, to calculate such an expression on a computer is an easy task.

[1] E. R. Th. Kerstel, K. K. Lehmann, T. F. Mentel, B. H. Pate, and G. Scoles, J. Phys. Chem. **95**, 8282 (1991).
[2] J. E. Gambogi, R. P. L'Esperance, K. K. Lehmann, B. H. Pate, and G. Scoles (to be published).
[3] R. E. Wyatt, Adv. Chem. Phys. **73**, 231 (1989).
[4] R. E. Wyatt, C. Iung, and C. Leforestier, J. Chem. Phys. **75**, 3458 (1992); **75**, 3477 (1992).
[5] T. Uzer, Phys. Rep. **199**, 73 (1991).
[6] M. L. Sage and J. Jortner, Adv. Chem. Phys. **47**, 293 (1981).
[7] K. V. Reddy, D. F. Heller, and M. J. Berry, J. Chem. Phys. **76**, 2814 (1982).
[8] M. E. Kellman, J. Phys. Chem. **87**, 2161 (1983).
[9] M. S. Child and L. Halonen, Adv. Chem. Res. **57**, 1 (1984).
[10] E. L. Sibert III, W. P. Reinhardt, and J. T. Hynes, J. Chem. Phys. **81**, 1115 (1984); **81**, 1135 (1984).
[11] T. Uzer, Chem. Phys. Lett. **110**, 356 (1984).
[12] S. Mukamel, J. Phys. Chem. **88**, 832 (1984).
[13] S. Mukamel and R. Islampur, Chem. Phys. Lett. **108**, 161 (1984).
[14] T. Uzer, Chem. Phys. Lett. **110**, 356 (1984).
[15] G. A. Voth and R. A. Marcus, J. Chem. Phys. **82**, 4064 (1985).
[16] K. N. Swamy and W. L. Hase, J. Chem. Phys. **84**, 361 (1985).
[17] D.-H. Lu, W. L. Hase, and R. J. Wolf, J. Chem. Phys. **85**, 4422 (1986).
[18] G. A. Voth, J. Phys. Chem. **90**, 3624 (1986).
[19] P. Hofmann, R. B. Garber, M. A. Ratner, L. C. Baylor, and E. Weitz, J. Chem. Phys. **88**, 7434 (1988).
[20] K. T. Marshall and J. S. Hutchinson, J. Chem. Phys. **95**, 3232 (1991).
[21] Y. F. Zhang and R. A. Marcus, J. Chem. Phys. **96**, 6065 (1992).
[22] A. A. Stuchebrukhov and R. A. Marcus (unpublished).
[23] M. J. Davis and E. J. Heller, J. Chem. Phys. **75**, 246 (1981); **75**, 3915 (1981).
[24] M. J. Davis and E. J. Heller, J. Phys. Chem. **85**, 307 (1981).
[25] E. L. Sibert III, W. P. Reinhardt, and J. T. Hynes, J. Chem. Phys. **77**, 3583 (1982).
[26] E. L. Sibert III, J. T. Hynes, and W. P. Reinhardt, J. Chem. Phys. **77**, 3595 (1982).
[27] K. Stefanski and E. Pollak, J. Chem. Phys. **87**, 1079 (1987).
[28] V. Lopez and R. A. Marcus, Chem. Phys. Lett. **93**, 232 (1982).
[29] K. N. Swamy and W. L. Hase, J. Chem. Phys. **82**, 123 (1985).
[30] V. Lopez, V. Fairen, S. M. Lederman, and R. A. Marcus, Chem. Phys. Lett. **75**, 3915 (1981).
[31] S. M. Lederman, V. Lopez, G. A. Voth, and R. A. Marcus, Chem. Phys. Lett. **124**, 93 (1986).
[32] S. M. Lederman, V. Lopez, V. Fairen, G. A. Voth, and R. A. Marcus, Chem. Phys. **139**, 171 (1989).
[33] T. Uzer and J. T. Hynes, Chem. Phys. **139**, 163 (1989).
[34] T. Uzer and J. T. Hynes, J. Phys. Chem. **90**, 3524 (1986).
[35] P. W. Anderson, Phys. Rev. **109**, 1492 (1958).
[36] P. Lee and T. V. Ramakrishnan, Rev. Mod. Phys. **57**, 287 (1985).
[37] D. E. Logan and P. G. Wolynes, J. Chem. Phys. **93**, 4994 (1990).
[38] A. Helman and R. A. Marcus, J. Chem. Phys. **95**, 872 (1991).
[39] J. S. Go, G. A. Bethardy, and D. S. Perry, J. Phys. Chem. **94**, 6153 (1990).

[40] M. Bixon and J. Jortner, J. Chem. Phys. **48**, 715 (1968); K. F. Freed and A. Nitzan, J. Chem. Phys. **73**, 4765 (1980).
[41] R. Haydock, in Solid State Physics, edited by H. Ehrenreich, F. Seitz, and D. Turnbull, (Academic, New York, 1980), Vol. 35, p. 215.
[42] J. F. Gaw, A. Willetts, W. H. Green, and N. C. Handy, in *Advances in Molecular Vibration and Collision Dynamics*, edited by J. M. Bowman (JAP Press, Greenwich, CT, 1990).
[43] G. A. Crowder, Vibration Spectrosc. **1**, 317 (1991).
[44] G. O. Carlisle, G. A. Crowder, Vibration. Spectrosc. **1**, 389 (1992).
[45] V. S. Nikitin, M. V. Polyakova, I. I. Baburina, A. V. Belyakov, E. T. Bogoradovskii, and V. S. Zavgorodnii, Spectrochimica Acta. **46A**, 1669 (1990).
[46] W. Zeil, J. Haase, and M. Dakkouri, Disc. Farad. Soc. **47**, 149 (1969).
[47] A. R. Hoy, I. M. Mills, and G. Strey, Mol. Phys. **24**, 1265 (1972).
[48] D. L. Duncan and M. M. Law, J. Molec. Spectrosc. **140**, 13, 1990.
[49] D. L. Duncan, Spectrochim. Acta **47A**, 1 (1991).
[50] W. D. Allen, Y. Yamaguchi, A. G. Császár, D. A. Clabo Jr, R. B. Remington, and H. F. Schaefer III, Chem. Phys. **145**, 427 (1990).
[51] M. Challacombe and J. Cioslowski, J. Chem. Phys. **95**, 1064 (1991).
[52] W. Schneider and W. Thiel, Chem. Phys. Lett. **157**, 367 (1989).
[53] J. L. Duncan, D. C. McKean, and G. D. Nivellini, J. Molec. Struct. **32**, 255 (1976).
[54] J. Esakov and T. Weiss, *Data Structures: An Advanced Approach Using C* (Prentice Hall, New York, 1989) [one of the present authors (RAM) disclaims any knowledge of C!].
[55] C. Duneczky and R. E. Wyatt, J. Chem. Phys. **89**, 1448 (1988); M. D'Mello, C. Duneczky, and R. E. Wyatt, Chem. Phys. **148**, 169 (1988); C. Duneczky and R. E. Wyatt, J. Phys. B **21**, 3727 (1988).
[56] M. D. Newton, Chem. Rev. **91**, 767 (1991).
[57] P. Siddarth and R. A. Marcus, J. Phys. Chem. **96**, 3213 (1992).
[58] K. K. Lehmann, private communication.
[59] M. L. Goldberger and K. M. Watson, *Collision Theory* (Wiley, New York, 1964).
[60] C. Manzanares, N. L. S. Yamasaki, and E. Weitz, J. Phys. Chem. **90**, 3953 (1986).